

Ladder-type Heteroarenes: Up to 15 Rings with Five Imide Groups

Yingfeng Wang⁺, Han Guo⁺, Shaohua Ling, Iratxe Arrechea-Marcos, Yuxi Wang, Juan Teodomiro López Navarrete, Rocio Ponce Ortiz,^{*} and Xugang Guo^{*}

Dedicated to Professor Tobin J. Marks

Abstract: A series of novel imide-functionalized ladder-type heteroarenes with well-defined structure and controllable conjugation lengths were synthesized and characterized. The synthetic route shows remarkable efficacy for constructing the electron-deficient ladder backbones. π -Conjugation extension leads to narrowed band gaps with enhanced electron affinities. The ladder arenes are incorporated into organic thin-film transistors, and show encouraging electron mobilities of 0.013–0.045 cm² V⁻¹ s⁻¹. The heteroarenes reported here provide a remarkable platform for fundamental physicochemical studies and materials innovation in organic electronics.

Organic π -conjugated materials are emerging semiconductors for next-generation optoelectronic devices, such as organic thin-film transistors (OTFTs) and organic solar cells (OSCs), owing to the advantages of low-cost, light-weight, and mechanical flexibility.^[1,2] The device performance of organic semiconductors is highly related to their backbone structure.^[3,4] In addition, intermolecular packing and film morphology on larger scale also play critical roles.^[5] Ladder-type molecules with highly planar backbones and well-delocalized π -conjugation have attracted intensive attention as small-molecule semiconductors and building blocks for polymers, molecular wires, and ladder polymers.^[6–19] Among them, pentacenes show substantial hole mobility,^[4] and benzothienobenzothiophene and dinaphthothienothiophene exhibit remarkable mobility with excellent OTFT stability.^[20,21] Recently, Bäuerle and co-workers reported the synthesis of a fused thiophene-pyrrole heterodecane by multiple aminations.^[22] A series of ladder-type thienoacenes based on benzodithiophene are synthesized, thus showing

interesting properties.^[23] However, most ladder-type molecules typically exhibit electron-rich characteristics^[6] and the synthesis of electron-deficient analogues remains a great challenge because of the reduced chemical reactivity and unfavored steric hindrance created by typical electron-withdrawing substituents.^[24–26] Hence it is highly imperative to develop electron-deficient ladder-type π -conjugated systems, which are highly desired for constructing donor-acceptor dyads^[27] and developing organic semiconductors using the donor-acceptor strategy.^[28]

Imide-functionalized arenes are highly promising π -conjugated materials,^[1,29] and the semiconductors derived from naphthalene diimide,^[30,31] perylene diimide,^[32] and thieno[3,4-c]pyrrole-4,6-dione^[33] are the representative materials in OTFT and OSC fields, thus showing highly encouraging device performance. Among various imide-functionalized arenes, the bithiophene imide (BTI, Figure 1) was first synthesized as an electron-deficient unit by Marks et al.,^[34] and its incorporation into polymers affords a series of semiconductors with remarkable performance in OTFTs and OSCs.^[35,36]

Inspired by the interesting physicochemical properties and encouraging device performance of ladder-type materials and the great success of imide-functionalized arenes, we herein report a series of novel imide-functionalized ladder-type heteroarenes BTI–BTI5 (Figure 1) with controllable

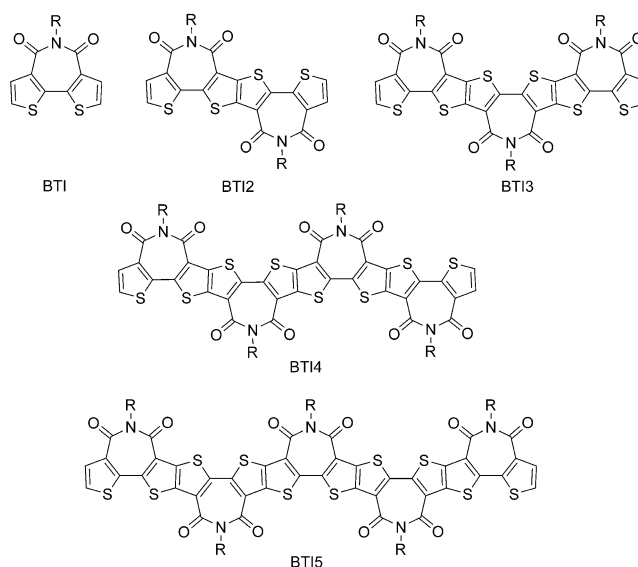


Figure 1. Chemical structures of the imide-functionalized ladder-type heteroarenes BTI–BTI5 with varied conjugation lengths.

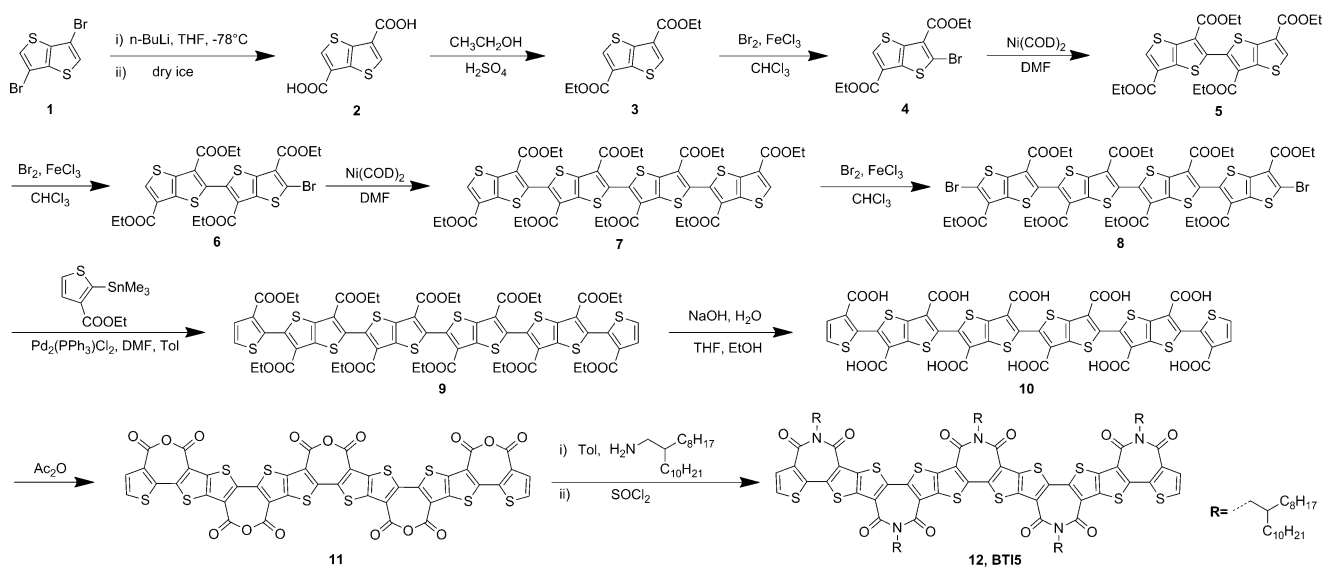
[*] Dr. Y. Wang,^[†] Dr. H. Guo,^[†] S. Ling, Y. Wang, Prof. X. Guo
Department of Materials Science and Engineering and The Shenzhen
Key Laboratory for Printed Organic Electronics
South University of Science and Technology of China
No. 1088, Xueyuan Road, Shenzhen, Guangdong 518055 (China)
E-mail: guoxg@sustc.edu.cn

I. Arrechea-Marcos, Prof. J. T. López Navarrete, Dr. R. P. Ortiz
Department of Physical Chemistry, University of Málaga
Campus de Teatinos s/n, 29071 Málaga (Spain)
E-mail: rocioponce@uma.es

Y. Wang
Department of Chemistry, Wuhan University
Wuhan, Hubei 430072 (China)

[†] These authors contributed equally to this work.

Supporting information and the ORCID identification number(s) for the author(s) of this article can be found under:
<https://doi.org/10.1002/anie.201702225>.



Scheme 1. Synthetic route to the ladder-type heteroarene BTI5 with 15 Rings and 5 imide groups.

conjugation lengths and varied BTI-fused heterocycles. The ladder-type arenes show excellent solubility, highly planar backbone, substantial crystallinity, and tunable optoelectrical properties. When tested in OTFTs, the BTI derivatives exhibit encouraging electron mobility.

Scheme 1 depicts the synthetic route to BTI5, the longest arene with 15 rings and 5 imide groups in a row, and it covers most reactions needed for the synthesis of the shorter BTI derivatives BTI2–BTI4 (see the Supporting Information). Palladium-catalyzed Stille coupling and/or nickel-mediated Yamamoto coupling are employed to construct the extended backbones. The construction of multiple imide groups is similar to the one used in the monoimide synthesis for BTI. Compared to the method developed for the BTI2 synthesis,^[37] the methyl ester is replaced with an ethyl ester to increase solubility and reaction yield, which are critical for the synthesis of the more extended BTI3–BTI5. One of the key steps is the monobromination of the compounds **3** and **5**, a step which is challenging because of the comparable reactivities at the α -positions on both ends of the molecules. It was found that the Br_2 addition conditions are critical, and Br_2 (1.0 equiv totally) addition in five different portions affords the monobrominated **4** and **6** in fair yield (40–50%) with about 20% unreacted starting material and about 20% of the dibrominated byproducts, which can be used for the synthesis of BTI2 and BTI3 (see the Supporting Information). By using the monobrominated **4**, both copper-mediated Ullmann coupling and palladium-catalyzed Stille coupling were attempted, but gave **5** in low yields (20–30%). To our delight, under nickel-mediated Yamamoto coupling, **4** and **6** can be successfully dimerized to afford **5** and **7**, respectively, in excellent yields (ca. 90%). The compound **7** is readily dibrominated using Br_2 to afford **8** in nearly quantitative yield, and it is then coupled with 2-(trimethylstannyl)thiophene-3-carboxylate to yield **9**. Hydrolysis in NaOH solution can readily convert the deca-ester **9** into the deca-acid **10** with remarkable yield (97%) and the subsequent dehydration affords the purple penta-anhydride **11** in excellent yield

(90%), and it is used for the following imidization without further purification because of its limited solubility. The thermodynamic nature of the ring-closing reaction favors the formation of ladder-type anhydrides.^[38,39]

Upon the synthesis of **11**, its full imidization becomes the key step. Fortunately, the imidization shows great success using a two-step protocol^[36] and toluene is chosen as the solvent in the alkylcarbamoyl-carboxylic acid formation step to increase the solubility and reaction temperature. The formed alkylcarbamoyl-carboxylic acid cannot be readily converted into the undesired dialkylcarbamoyl (or diamide) under these reaction conditions, which is critical for the imide synthesis. The multiple reaction sites on the penta-anhydride **11** result in a variety of carbamoyl-carboxylic acid isomers, which are difficult to purify and characterize. Without further purification, the isomers are subjected to SOCl_2 -assisted cyclization to afford the penta-imide **12** in 20% overall yield. The moderate yield is likely due to the unpurified anhydride **11**. In contrast, it was found that the iminochloride byproduct^[40] is formed and the byproduct yield gets higher as the anhydride number increases. As a result, imidization results in greatly improved yields for the shorter BTI derivatives, which are 37%, 49%, 76%, and 90% for BTI4, BTI3, BTI2, and BTI, respectively (see the Supporting Information). In addition, BTI–BTI5 can be readily brominated, and thus enables materials development by incorporating these novel electron-deficient units into small molecules and polymer semiconductors.

In spite of the high efficacy for the synthesis of these ladder-type BTI derivatives, we must admit that the synthetic route to the longest BTI5 is tedious. In contrast, the nickel-mediated Yamamoto coupling is remarkably powerful for backbone extension, and has also been used for the synthesis of BTI-based homopolymers.^[35] The synthesis of BTI-based ladder-type polymers is ongoing in our lab and we expect that high-quality ladder polymers are achievable if quantitative postpolymerization imidization can be realized.

All ladder-type heteroarenes show ready solubility at room temperature, even for the longer BTI4 and BTI5 with solubilities of 14 and 13 mg mL⁻¹, respectively, in chloroform. The chemical structures of BTI–BTI5 were confirmed by NMR spectra, MALDI-TOF mass spectra (Figure 2), high-resolution mass spectrometry (HRMS), and elemental analysis (see the Supporting Information). Among the series, BTI,

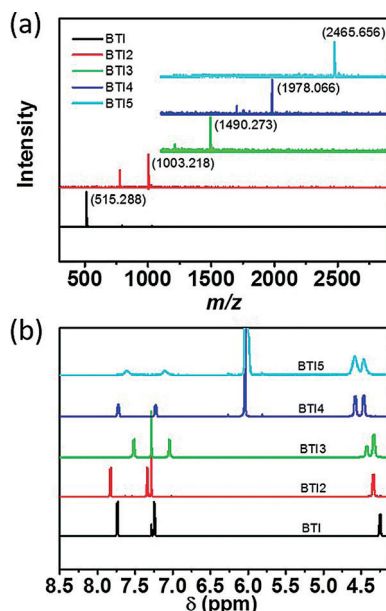


Figure 2. a) MALDI-TOF mass spectra and b) ¹H NMR spectra (in aromatic region) of BTI–BTI5. CDCl₃ is used for NMR measurements of BTI–BTI3 at room temperature and C₂Cl₄D₂ is used for BTI4 and BTI5 at 120 °C.

BTI2, and BTI3 show well-resolved NMR chemical shifts, however the longer BTI4 and BTI5 cannot achieve high-quality ¹H NMR signals at room temperature because of their strong aggregation induced by the extended ladder π -systems. At 120 °C, the NMR spectra (Figure 2b) of BTI4 and BTI5 show improved resolution. It is interesting to note that on the basis of the HMRS spectra of BTI4 and BTI5 (see Figures S64 and S65 in the Supporting Information), the isotope peaks indicate that z should be equal to +2, therefore m is double the molecular weights of BTI4 and BTI5. Although the exact reason for such HMRS spectra is unknown at this stage, we speculate that the doubled m value is likely due to the formation of BTI4 and BTI5 dimers induced by their strong intermolecular interactions, and is in good accordance with their UV-vis absorption and NMR measurement. Cultivation of single crystals of BTI2–BTI5 failed because of the long and branched side chains and the analogues with straight chains show limited solubility.

The optical properties of these heteroarenes are investigated by measuring their absorption spectra (Figure 3). The absorption onsets in chlorobenzene show a gradual bathochromic shift from $\lambda = 390$ nm for BTI to $\lambda = 637$ nm for BTI5 (Figure 3a), and the films exhibit similar transition with the decreased optical gaps (Figure 3c). At room temperature BTI2–BTI4 show absorption spectra with a vibrationally

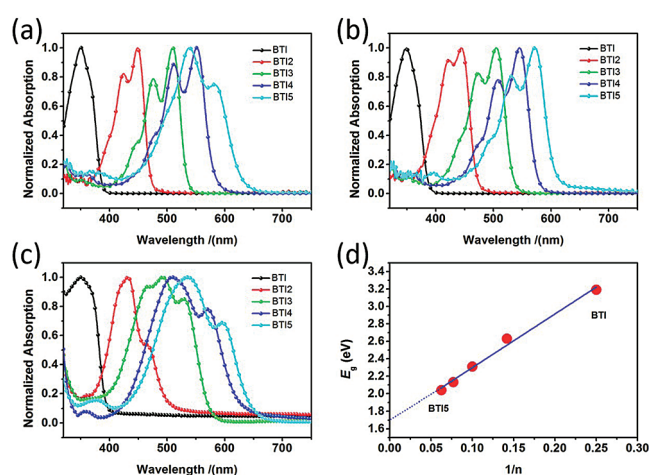


Figure 3. Absorption spectra of a) BTI–BTI5 solutions in chlorobenzene at 298 K; b) BTI–BTI5 solutions in chlorobenzene at 373 K; c) BTI–BTI5 films. d) Optical gap of BTI–BTI5 in correlation with the reciprocal number of double bonds. The optical gap is derived from BTI–BTI5 absorption in solution at 373 K.

structured absorption shoulder and a sharp absorption edge as expected for ladder-type oligomers.^[7–9] However on the basis of the absorption spectra in solution and film state, BTI5 shows distinctive aggregation in solution at room temperature. As the temperature is increased to 373 K, BTI5 then de-aggregates. For more consistent comparison, the absorption onsets of BTI–BTI5 solutions at 373 K (Figure 3b) are used for the calculation of optical gaps since all chromophores are in isolated form. The optical gaps decrease from 3.19 eV for BTI to 2.04 eV for BTI5 and correlate linearly with the reciprocal number of double bonds with a correlation coefficient of 0.995 (Figure 3d).^[22] Such a linear correlation is in agreement with theoretical calculations (see Figure S5). The limit of the extrapolated optical gap is about 1.7 eV, thus showing good tunability from wide to medium optical gaps by backbone extension. The thermal properties of BTI–BTI5 are studied by thermogravimetric analysis (TGA) and the TGA curves exhibit excellent stability with the decomposition temperatures typically larger than 450 °C, except for BTI (see Figure S2). Hence as the conjugation length increases, the thermal stability is enhanced and then saturates for these ladder-type arenes.

Electrochemical properties of BTI–BTI5 were investigated by cyclic voltammetry (CV) with referencing to a ferrocene/ferrocenium (Fc/Fc⁺) internal standard (see Figure S1). The onsets of reduction potentials are –2.07, –1.46, –1.21, –1.10, and –0.81 V for BTI, BTI2, BTI3, BTI4, and BTI5, respectively. Hence with the π -conjugation extension, the derived LUMOs are gradually decreased from –2.29 eV for BTI to –3.55 eV for BTI5, thus indicating increased electron affinity. The gradual decrement trend of the LUMOs is in good accord with the results from theoretical calculations, where a stabilization of about 1 eV is recorded on going from BTI to BTI5. On the contrary, the experimentally derived HOMOs partially differ from the trend extracted from DFT calculations, and is likely due to its tendency to overestimate conjugation. The CV data render similar

HOMOs for BTI–BTI5, while a HOMO destabilization of about 0.6 eV is found theoretically from BTI to BTI5. Hence, HOMOs seems to be less affected than LUMOs with chain lengthening (Figure 4a). The results indicate that the band-gap lowering is mainly attributed to the decreased LUMOs

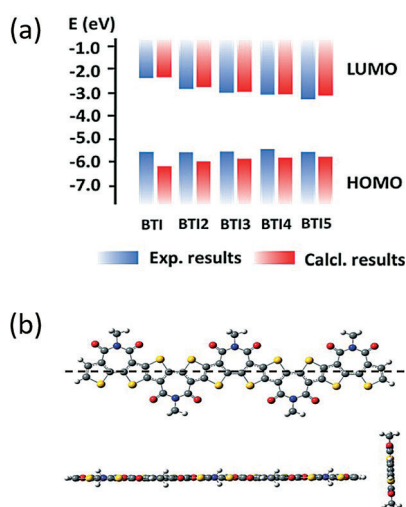


Figure 4. a) Experimentally measured and B3LYP/6-31G** calculated FMO energy levels of BTI–BTI5. b) B3LYP/6-31G** optimized BTI5 geometry.

with extended conjugation, and contrasts from previous reports, wherein the main contribution to band-gap lowering was from the HOMO or both HOMO and LUMO in these kinds of ladder-type arenes.^[22,23] The DFT optimized energies show highly planar backbones for all these ladder-type arenes, with dihedral angles of less than 1° (Figure 4b; see Figure S6), and in good accord with the BTI single-crystal structure. In addition, the DFT calculations reveal a straight BTI5 backbone (Figure 4b). The planar and straight backbones are beneficial to materials packing and film ordering.

Internal reorganization energies were computed for all these ladder-type arenes. As expected, for both hole and electron transport the energies decrease substantially in the longest derivatives (see the Supporting Information), because of delocalization of the injected charge over a larger number of conjugated C–C/C=C bonds. Please note that the decrease is significant for electron transport on going from BTI (0.40 eV) to BTI2 (0.26 eV) and to BTI3 (0.22 eV). However it stays quite balanced for the longer systems, at 0.20 and 0.18 eV for BTI4 and BTI5, respectively. These data are in good agreement with the DFT-derived LUMO topologies which show an electron density confinement in the central parts of BTI4 and BTI5, thus rendering a similar extension (see Figure S6). To further analyze the conjugation extension, FT-Raman spectra were recorded for BTI–BTI5 (see Figure S3). The most intense Raman mode, which is ascribed to a symmetric $\nu(\text{C}=\text{C}/\text{C}-\text{C})$ vibration, and can be related to line B in linear oligothiophenes, gives valuable information on the conjugated extension. This band downshifts from 1470 cm^{-1} for BTI to 1451 cm^{-1} for BTI5. This modest shift with chain elongation is similar to that observed for linear oligothiophenes.^[41]

Focusing on the second most intense band, whose theoretical eigenvector indicates that it arises from an in-phase antisymmetric $\nu(\text{C}=\text{C})$ mostly localized on the outer rings, a notable downshift of 30 cm^{-1} is recorded on going from BTI (1553 cm^{-1}) to BTI3 (1523 cm^{-1}). However, it stays unaltered for longer chains (see Figures S7–10). This Raman mode can be related to the well-known line A of linear oligothiophenes, which is remarkably sensitive to conjugation length.^[41] Note however that the most intense band is still slightly downshifted for BTI5. Therefore, the results obtained here indicate that although the band gaps are still diminishing and some conjugation changes are still evidenced by Raman spectra, we are reaching saturation at the longer analogues BTI3–BTI5, and it is in good accord with the trend in Figure 3d and the localization of the LUMO orbital topologies in the central part of the conjugated skeleton, with modest contribution of the external rings for BTI4 and BTI5 (see Figure S6). All the above evidence indicates that electron delocalization, a key parameter in charge transport, may be quite similar for BTI3–BTI5. Thus, synthesizing longer fused systems may not be necessary, in terms of π -conjugation.

Top-gate/bottom-contact OTFTs were fabricated to investigate the potential applications of these building blocks in organic electronics. The OTFTs of all these ladder-type BTI derivatives show encouraging electron-transporting characteristics with average electron mobilities of 0.013–0.045 $\text{cm}^2 \text{V}^{-1} \text{s}^{-1}$ in the saturated regime (see Tables S3 and S4) except BTI. The inactivity of BTI OTFTs is attributed to no quality film formation and substantial charge carrier injection barrier. The representative transfer curve of BTI5 OTFTs (Figure 5b) shows a “kink-free” feature, and is indicative of the reliability of these mobility values. From BTI2 to BTI4, the threshold voltage (V_t) gradually decreases, and is in good accordance with the LUMO evolution. As the backbone extends, in addition to n-channel performance, the longest BTI5 exhibits p-channel performance with a hole mobility of more than $10^{-3} \text{cm}^2 \text{V}^{-1} \text{s}^{-1}$. It should be pointed

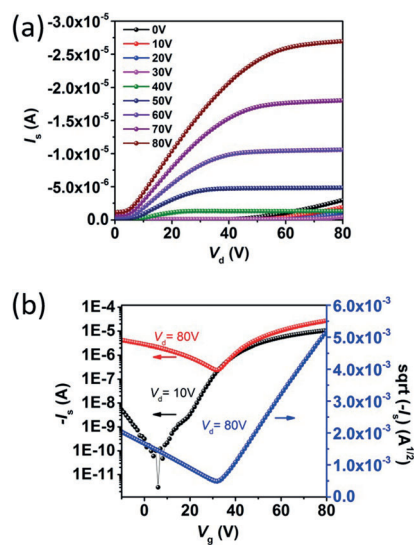


Figure 5. a) Output and b) transfer characteristics of BTI5 OTFTs. The active layer is deposited from solution.

out that all these BTI derivatives contain very bulky 2-octyldodecyl side chains, which are detrimental to molecule packing, and thus with side chain engineering and more intensive device optimization, improved OTFT performance can be expected. The results clearly demonstrate the great potentials of these ladder-type imide-functionalized heteroarenes for n-type semiconductors.

To conclude, we have successfully synthesized a series of novel imide-functionalized ladder-type heteroarenes with up to 5 imide groups and 15 rings in a row. The synthetic route shows remarkable efficacy for constructing ladder-type backbones with multiple imide functionalities. These fused arenes exhibit excellent solubilities, highly planar backbones, substantial crystallinity, and tunable conjugation lengths and optoelectrical properties. Compared to most fused arenes, these novel imide-functionalized arenes are highly electron-deficient. As the backbone extends, the band gap is diminishing, but the longest BTI5 approaches saturation. Hence synthesizing longer fused systems may not be necessary in terms of π -conjugation and charge carrier stabilization. As a proof of materials design, the BTI derivatives show promising electron-transport properties. The results herald the great potentials of these imide-functionalized ladder-type arenes for small-molecule semiconductors and as a class of building blocks for high-performance polymers.

Acknowledgments

X.G. thanks NSFC (51573076), Shenzhen Peacock Plan (KQTD20140630110339343), Shenzhen Basic Research Fund (JCYJ20160530185244662), Shenzhen Key Lab funding (ZDSYS201505291525382). H.G. is grateful to Shenzhen Basic Research Fund (JCYJ20160530190226226). Research at Malaga was supported by MINECO (CTQ2015-66897-P). R.P.O. and I.A.-M. thank the MINECO for a Ramón y Cajal research contract and for a predoctoral fellowship, respectively. S.L. acknowledges the USI Training Program (2016S11).

Conflict of interest

The authors declare no conflict of interest.

Keywords: conjugation · heteroarenes · ladder polymers · semiconductors · structure–activity relationships

- [1] J. Zaumseil, H. Sirringhaus, *Chem. Rev.* **2007**, *107*, 1296–1323.
- [2] X. Guo, A. Facchetti, T. J. Marks, *Chem. Rev.* **2014**, *114*, 8943–9021.
- [3] K. Takimiya, S. Shinamura, I. Osaka, E. Miyazaki, *Adv. Mater.* **2011**, *23*, 4347–4370.
- [4] J. E. Anthony, *Chem. Rev.* **2006**, *106*, 5028–5048.
- [5] F. J. M. Hoeben, P. Jonkheijm, E. W. Meijer, A. P. H. J. Schenning, *Chem. Rev.* **2005**, *105*, 1491–1546.
- [6] H. Tsuji, E. Nakamura, *Acc. Chem. Res.* **2017**, *50*, 396–406.

- [7] J. Grimme, M. Kreyenschmidt, F. Uckert, K. Müllen, U. Scherf, *Adv. Mater.* **1995**, *7*, 292–295.
- [8] F. Schindler, J. Jacob, A. C. Grimsdale, U. Scherf, K. Müllen, J. M. Lupton, J. Feldmann, *Angew. Chem. Int. Ed.* **2005**, *44*, 1520–1525; *Angew. Chem.* **2005**, *117*, 1544–1549.
- [9] J. Grimme, U. Scherf, *Macromol. Chem. Phys.* **1996**, *197*, 2297–2304.
- [10] B. S. Nehls, S. Földner, E. Preis, T. Farrell, U. Scherf, *Macromolecules* **2005**, *38*, 687–694.
- [11] J. D. Plumbhof, T. Stöferle, L. Mai, U. Scherf, R. F. Mahrt, *Nat. Mater.* **2014**, *13*, 247–252.
- [12] K. J. Kass, M. Forster, U. Scherf, *Angew. Chem. Int. Ed.* **2016**, *55*, 7816–7820; *Angew. Chem.* **2016**, *128*, 7947–7951.
- [13] A. Babel, S. A. Jenekhe, *J. Am. Chem. Soc.* **2003**, *125*, 13656–13657.
- [14] J.-S. Wu, S.-W. Cheng, Y.-J. Cheng, C.-S. Hsu, *Chem. Soc. Rev.* **2015**, *44*, 1113–1154.
- [15] J. Lee, A. J. Kalin, T. Yuan, M. Al-Hashimic, L. Fang, *Chem. Sci.* **2017**, *8*, 2503–2521.
- [16] C. Zhu, Z. Guo, A. U. Mu, Y. Liu, S. E. Wheeler, L. Fang, *J. Org. Chem.* **2016**, *81*, 4347–4352.
- [17] Y. Zou, X. Ji, J. Cai, T. Yuan, D. J. Stanton, Y. Lin, M. Naraghi, L. Fang, *Chem* **2017**, *2*, 139–152.
- [18] A. L. Briseno, S. C. B. Mannsfeld, P. J. Shamberger, F. S. Ohuchi, Z. Bao, S. A. Jenekhe, Y. Xia, *Chem. Mater.* **2008**, *20*, 4712–4719.
- [19] G. E. Rudebusch, J. L. Zafra, K. Jorner, K. Fukuda, J. L. Marshall, I. Arrechea-Marcos, G. L. Espejo, R. P. Ortiz, C. J. Gómez-García, L. N. Zakharov, M. Nakano, H. Ottosson, J. Casado, M. M. Haley, *Nat. Chem.* **2016**, *8*, 753–759.
- [20] T. Mori, T. Nishimura, T. Yamamoto, I. Doi, E. Miyazaki, I. Osaka, K. Takimiya, *J. Am. Chem. Soc.* **2013**, *135*, 13900–13913.
- [21] K. Niimi, S. Shinamura, I. Osaka, E. Miyazaki, K. Takimiya, *J. Am. Chem. Soc.* **2011**, *133*, 8732–8739.
- [22] C. Wetzel, E. Brier, A. Vogt, A. Mishra, E. Mena-Osteritz, P. Bäuerle, *Angew. Chem. Int. Ed.* **2015**, *54*, 12334–12338; *Angew. Chem.* **2015**, *127*, 12511–12515.
- [23] T. Zheng, Z. Cai, R. Ho-Wu, S. H. Yau, V. Shaparov, T. Goodson, L. Yu, *J. Am. Chem. Soc.* **2016**, *138*, 868–875.
- [24] F. Würthner, V. Stepanenko, Z. Chen, C. R. Saha-Möller, N. Kocher, D. Stalke, *J. Org. Chem.* **2004**, *69*, 7933–7939.
- [25] X. Gao, C. Di, Y. Hu, X. Yang, H. Fan, F. Zhang, Y. Liu, H. Li, D. Zhu, *J. Am. Chem. Soc.* **2010**, *132*, 3697–3699.
- [26] A. H. Endres, M. Schaffroth, F. Paulus, H. Reiss, H. Wadepohl, F. Rominger, R. Krämer, U. H. F. Bunz, *J. Am. Chem. Soc.* **2016**, *138*, 1792–1795.
- [27] P. E. Hartnett, C. M. Mauck, M. A. Harris, R. M. Young, Y.-L. Wu, T. J. Marks, M. R. Wasielewski, *J. Am. Chem. Soc.* **2017**, *139*, 749–756.
- [28] J. Roncali, *Chem. Rev.* **1997**, *97*, 173–206.
- [29] X. Zhan, A. Facchetti, S. Barlow, T. J. Marks, M. A. Ratner, M. R. Wasielewski, S. R. Marder, *Adv. Mater.* **2011**, *23*, 268–284.
- [30] T. He, M. Stolte, C. Burschka, N. H. Hansen, T. Musiol, D. Kälblein, J. Pflaum, X. Tao, J. Brill, F. Würthner, *Nat. Commun.* **2015**, *6*, 5954.
- [31] H. Yan, Z. Chen, Y. Zheng, C. Newman, J. R. Quinn, F. Dotz, M. Kastler, A. Facchetti, *Nature* **2009**, *457*, 679–686.
- [32] W. Jiang, Y. Li, Z. Wang, *Acc. Chem. Res.* **2014**, *47*, 3135–3147.
- [33] Y. Zou, A. Najari, P. Berrouard, S. Beaupré, B. Rédaïchi, Y. Tao, M. Leclerc, *J. Am. Chem. Soc.* **2010**, *132*, 5330–5331.
- [34] J. A. Letizia, M. R. Salata, C. M. Tribout, A. Facchetti, M. A. Ratner, T. J. Marks, *J. Am. Chem. Soc.* **2008**, *130*, 9679–9694.
- [35] X. Guo, R. P. Ortiz, Y. Zheng, Y. Hu, Y.-Y. Noh, K.-J. Baeg, A. Facchetti, T. J. Marks, *J. Am. Chem. Soc.* **2011**, *133*, 1405–1418.
- [36] X. Guo, N. Zhou, S. J. Lou, J. Smith, D. B. Tice, J. W. Hennek, R. P. Ortiz, J. T. L. Navarrete, S. Li, J. Strzalka, L. X. Chen,

- R. P. H. Chang, A. Facchetti, T. J. Marks, *Nat. Photonics* **2013**, *7*, 825–833.
- [37] M. Saito, I. Osaka, Y. Suda, H. Yoshida, K. Takimiya, *Adv. Mater.* **2016**, *28*, 6921–6925.
- [38] J. Lee, B. B. Rajeeva, T. Yuan, Zi. Guo, Y. Lin, M. Al-Hashimi, Y. Zheng, L. Fang, *Chem. Sci.* **2016**, *7*, 881–889.
- [39] Y. Yao, J. M. Tour, *Macromolecules* **1999**, *32*, 2455–2461.
- [40] C. J. Ohnmacht, C. W. Draper, R. F. Dedinas, P. Loftus, J. J. Wong, *J. Heterocycl. Chem.* **1983**, *20*, 321–329.
- [41] J. Casado, S. Hotta, V. Hernández, J. T. López Navarrete, *J. Phys. Chem. A* **1999**, *103*, 816–822.

Manuscript received: March 1, 2017

Revised manuscript received: May 30, 2017

Version of record online: ■ ■ ■ ■, ■ ■ ■ ■ ■

Communications



Polymers

Y. Wang, H. Guo, S. Ling,
I. Arrechea-Marcos, Y. Wang,
J. T. López Navarrete, R. P. Ortiz,*
X. Guo* ————— ■■■■-■■■■

Ladder-type Heteroarenes: Up to 15
Rings with Five Imide Groups



Climbing the ladder: A series of novel ladder-type heteroarenes with well-defined structures and precisely controllable conjugation lengths were synthesized with remarkable efficacy and characterized. Compared to most ladder-type arenes, these imide-functionalized building blocks are highly electron-deficient, and thus provide a remarkable platform for materials innovation in organic electronics.